Influence of surface roughness on the infrared reststrahlen band

1995 J. Phys.: Condens. Matter 7 7173

(http://iopscience.iop.org/0953-8984/7/36/007)

J. Phys.: Condens. Matter 7 (1995) 7173–7184. Printed in the UK

Influence of surface roughness on the infrared reststrahlen band

Stefan K Andersson and Gunnar A Niklasson

Solid State Physics, Department of Technology, Box 534, Uppsala University, S-751 21 Uppsala, Sweden

Received 24 February 1995

Abstract. We study the influence of surface roughness on the infrared reststrahlen band in insulating materials. We model the surface features with either truncated spherical bumps on, or truncated spherical pits in, the substrate. The polarizability of the truncated sphere–substrate system has been calculated from a multipolar expansion, taking into account up to 16 orders. Two types of resonance have been identified. Substrate-related absorption peaks occur at the transverse optical or longitudinal optical phonon frequency, depending on the direction of the incident electric field. Additional absorption peaks occur in the vicinity of the resonance frequency of a sphere. They are dependent on the detailed geometrical configuration.

1. Introduction

The infrared-optical properties of ionic materials are dominated by the so-called reststrahlen band between the transverse optical (TO) phonon frequency ω_T and longitudinal optical (LO) phonon frequency ω_L. Transverse electromagnetic waves can interact with transverse optical phonons and the quantum of the coupled field is called a polariton. In the reststrahlen region the real part of the dielectric function is negative, which leads to a high reflectance from the surface of a slab of the material, which leads to a high reflectance from the surface of a slab of the material. In addition the material is strongly absorbing, and the imaginary part of the dielectric function exhibits a resonance at the transverse optical phonon frequency.

In the case of small crystallites of ionic material, the position of the polariton resonance depends on their size and shape [1]. The situation is particularly simple for particles that are much smaller than the wavelength of the incident electromagnetic field. In the case of spheres, Fröhlich [2] showed that the resonance peak occurs at a frequency ω_F, between the TO and LO frequencies. This is also the case for ellipsoids [3], but here one peak is obtained for each of the three depolarization factors that describe the shape of the ellipsoid.

Roughness in the form of protrusions from and pits in the surface modifies the features in the reststrahlen band significantly. These effects were first studied by Berreman [4], who modelled the surface roughness with hemispherical bumps and pits. He showed that structure appears in the reststrahlen band, because of excitation of resonances associated with the surface inhomogeneities. A similar method has been used to calculate the electric field at a bump on a metal surface [5]. In the case of surface features that are much smaller than the wavelength, quasi-static theories for a variety of shapes now exist. This is mainly due to the efforts of the Leiden group, who have treated the optical properties of truncated spheres [6, 7] and spheroids [8] on a substrate. Their theory has, to our knowledge, not been applied to the reststrahlen band, however.

0953-8984/95/367173+12$19.50

In this paper we present the results of extensive quasi-static calculations of the polarizability of truncated spheres on, and truncated spherical pits in, the surface of an ionic material. Some results on prolate and oblate spheroids are also included. Of the currently solvable geometries, the truncated sphere is regarded as the best approximation to a real rough surface. Knowledge of the shape dependence of the features in the reststrahlen band is important for the interpretation of experiments on various ionic or partly ionic solids. The present study was motivated by the observation of an extra dip in the reststrahlen bands of ceramic beryllium oxide and silicon carbide. This feature was interpreted as being due to the effects of surface irregularities [9]. In section 2 below, we briefly review the theory behind our calculations. First the analytical solution for a small sphere and a sphere on a surface in the dipolar approximation are recalled. Then we shortly describe the theory of Vlieger and co-workers [6–8] for truncated spheres and spheroids. These theories can also, with proper modifications, be used for pits in the material. The results from our calculations for truncated spheres on, and truncated pits in, the surface are presented in section 3. A detailed study of the shape dependence on the strength and position of the resonance peaks is described. In section 4 we present some concluding remarks.

2. Theory

2.1. Free ellipsoidal particles

Consider a free ellipsoid with one of the principal axes parallel to the direction of the incident light. If the ellipsoid is much smaller than the wavelength, the polarizability may be written as [3, 10]

$$\alpha = \frac{\epsilon_m(\epsilon - \epsilon_m)}{\epsilon_m + L(\epsilon - \epsilon_m)} V \tag{1}$$

where V is the volume of the ellipsoid, ϵ and ϵ_m are the dielectric functions of the ellipsoid and the ambient, respectively, and L is the depolarization factor, a dimensionless number between 0 and 1. A triplet of depolarization factors describe the shapes of the ellipsoid, and their sum is unity. For a sphere, obviously, $L = 1/3$.

Equation (1) yields that the imaginary part of the polarizability has a resonance for $\epsilon = \epsilon_m(1 - 1/L)$. The condition $0 < L < 1$ ensures that the resonance appears when $\epsilon < 0$. In the case of an insulator, this occurs only inside the reststrahlen band between ω_T and ω_L. For a randomly oriented ellipsoid, three resonances are obtained, which correspond to the three principal axes.

2.2. Particles at the surface: the dipole approximation

If the particle is in contact with the substrate, the interaction between the electromagnetic field and the material is more complicated. In this section we consider the special case of a sphere on a substrate. This problem can be solved by expanding the electrical potential into multipoles. The dipole approximation yields the following expression for the polarizability of a sphere on a substrate [7]:

$$\alpha_\perp = \frac{\epsilon_m(\epsilon - \epsilon_m)}{\epsilon_m + L_\perp(\epsilon - \epsilon_m)} V \tag{2}$$

$$\alpha_\parallel = \frac{\epsilon_m(\epsilon - \epsilon_m)}{\epsilon_m + L_\parallel(\epsilon - \epsilon_m)} V. \tag{3}$$

Here $\alpha_\perp$ and $\alpha_\parallel$ are the polarizabilities of the sphere when the electric field E is perpendicular and parallel, respectively, to the surface of the substrate. The particle volume is denoted by V, and $L_\perp$ and $L_\parallel$ are effective depolarization factors given by

$$L_\perp = \frac{1}{3}\left[1 - \frac{\epsilon_{sub} - \epsilon_m}{4(\epsilon_{sub} + \epsilon_m)}\right] \tag{4}$$

$$L_\parallel = \frac{1}{3}\left[1 - \frac{\epsilon_{sub} - \epsilon_m}{8(\epsilon_{sub} + \epsilon_m)}\right]. \tag{5}$$

Here ϵ_{sub} is the dielectric function of the substrate. As in the case of a free ellipsoid, the imaginary polarizability has resonances for $\epsilon = \epsilon_m(1 - 1/L_{\perp,\parallel})$. If the particle and the substrate have equal dielectric functions, the absorption has two resonances for each direction of the electric field E. If the electric field is parallel to the surface of the substrate, these resonances occur for $\epsilon = 3\epsilon_m$ and $\epsilon = 5/7\epsilon_m \approx -0.71\epsilon_m$. When E is perpendicular to the surface of the substrate, the imaginary part of the polarizability has maxima for $\epsilon \approx -4.1\epsilon_m$ and $\epsilon \approx -0.57\epsilon_m$. For a free sphere the resonance, i.e. the Fröhlich [2] model, occurs at $\epsilon = -2\epsilon_m$.

2.3. General theory

In this section we briefly describe the general theory of Vlieger and co-workers [6–8], for particles much smaller than the wavelength, and situated at a surface. In this quasi-static limit, the electric potential is obtained from a solution of the Laplace equation.

Consider a truncated sphere on a substrate, as depicted in figure 1. We introduce a truncation parameter $r_0 = d/R$, where d is the distance between the centre of the sphere and the substrate. If the centre is situated under the surface of the substrate, r_0 is negative. If the centre is situated above the substrate, r_0 is positive. A homogeneous electric field is incident from the ambient medium 1. The Laplace equation has to be solved in the ambient 1, in the substrate 2, in the truncated sphere 3 and in the region 4 in the substrate.

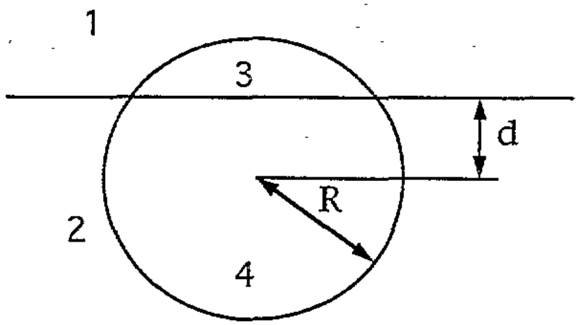

Figure 1. Cross section of a truncated sphere on a substrate. The numbers 1–4 denote the four regions, where the Laplace equation has to be solved.

In order to solve this problem, we expand the electrical potential into multipoles and image multipoles. The electrical potential can then be divided into three parts:

$$\psi_{tot} = \psi_{ext} + \sum_{l=1} \psi_l + \sum_{l'=1} \psi'_{l'} \tag{6}$$

where ψ_{ext} is the potential due to the external electric field, and the second and third terms give the contributions to the potential due to multipoles induced in the sphere and due to image multipoles, respectively. Because of symmetry the image multipoles are situated at the distance 2d from the centre of the sphere. If the centre of the sphere is above the surface of the substrate, the image multipoles are situated in the substrate and the reverse. The use of multipoles makes it easy to satisfy the boundary conditions at the spherical surface, and leads to an infinite set of linear inhomogeneous equations for the multipole coefficients. A technique for solving these equation has been given in [6, 7]. In practice, one takes into account the N first equations to obtain the N first multipole coefficients. Subsequently the polarizabilities $\alpha_{\parallel}$ and $\alpha_{\perp}$ are calculated numerically. They are proportional to the dipole coefficients but include contributions from the N first multipoles. Bobbert and Vlieger [8] have employed a similar method for the case of a spheroid on a substrate, by use of spheroidal multipoles.

It is possible to use the same theory to carry out calculations for pits and holes in the substrate. This is accomplished by dividing all the dielectric functions in this geometry by the dielectric function of the substrate [11]. In this way the pit or hole is transformed into a truncated sphere or spheroid with $\epsilon' = \epsilon_m/\epsilon_s$. The ambient now becomes the substrate with the above value of ϵ', while the substrate becomes the ambient with $\epsilon = 1$. One must also multiply the estimated polarizability by minus one because the angle of incidence of the electric field is changed by π.

In this paper we use these theories in order to investigate the influence of the shape of surface features on the reststrahlen band in the infrared. In our calculations we have included all multipoles up to $N = 16$. In the case of touching particles, or particles touching a substrate, the convergence of the multipolar expansion is a difficult issue. Haarmans and Bedeaux [12] have investigated the convergence for the case of a metal sphere on a transparent substrate. For low coverages they find that 15–19 multipoles are necessary to obtain an accuracy of 10^{-5}. The situation that we consider is a little different, however. In the reststrahlen band, ionic materials have dielectric functions of 'metallic' character. Work on touching metallic particles indicates that the multipole expansion exhibits a very slow convergence in this case [13]. However, expansions with multipoles up to $N = 8$ give a good qualitative picture of the optical response [14].

We have tested the convergence in our case by using different values of N. We found that convergence is obtained with $N = 16$ when $r_0 < 0$ but, when $r_0 > 0$, convergence was not complete even with $N = 16$. However, the discussion above indicates that our calculations should give qualitatively correct results even in this case, although small peak shifts and some peak broadening might be expected from the effects of higher multipoles.

3. Results and discussion

3.1. Calculations

In this paper we study the optical phonon absorption between ω_T and ω_L for insulators with rough surfaces. The optical constants for BeO [15] are used in this work, but the resonance effects are general for all ionic or partly ionic materials. For beryllia, the wavelength of the transverse optical mode is 14.1 μm and the wavelength of the longitudinal optical mode is 9.1 μm.

Calculations have been carried out for oblate and prolate spheroids at the surface of the substrate and for truncated spheres and holes. The imaginary part of the polarizability per unit particle volume is shown for different geometries and for different directions of the

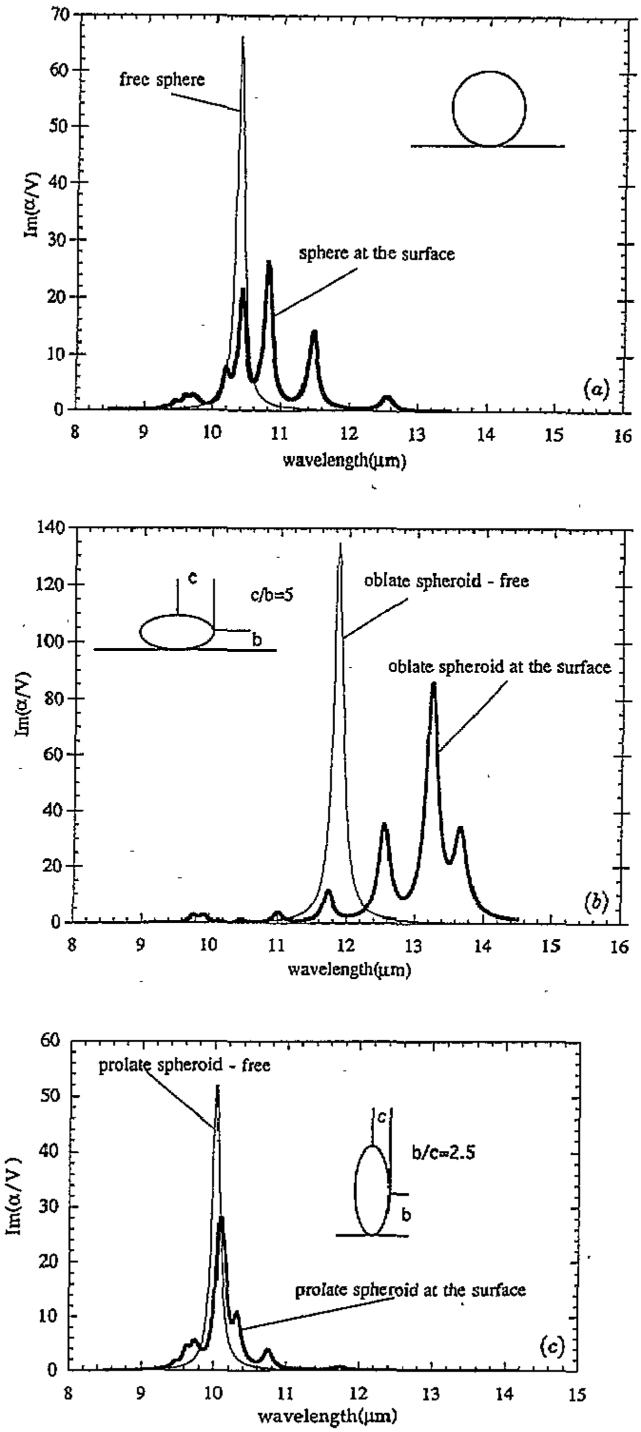

Figure 2. The imaginary polarizability per unit volume versus wavelength, for the electric field parallel to the substrate for (a) a sphere, (b) an oblate spheroid and (c) a prolate spheroid.

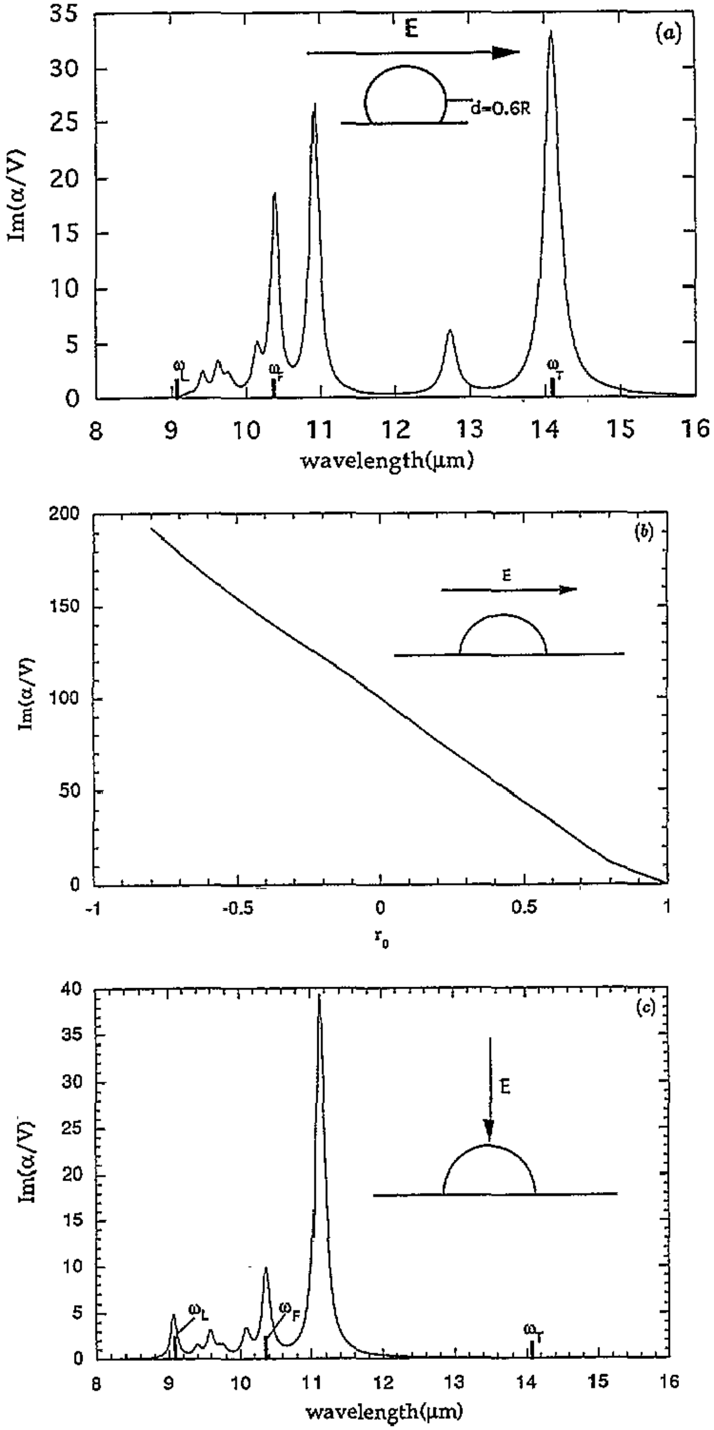

Figure 3. (a) The imaginary polarizability per unit volume versus wavelength for a truncated sphere with $r_0 = 0.6$ at the substrate surface. E was parallel to the substrate. (b) The maximum imaginary polarizability per unit volume for the substrate-related resonance at ω_T in (a) versus the truncation parameter r_0. (c) The imaginary polarizability per unit volume versus wavelength for a truncated sphere with $r_0 = 0$ at the substrate surface. E was perpendicular to the substrate.

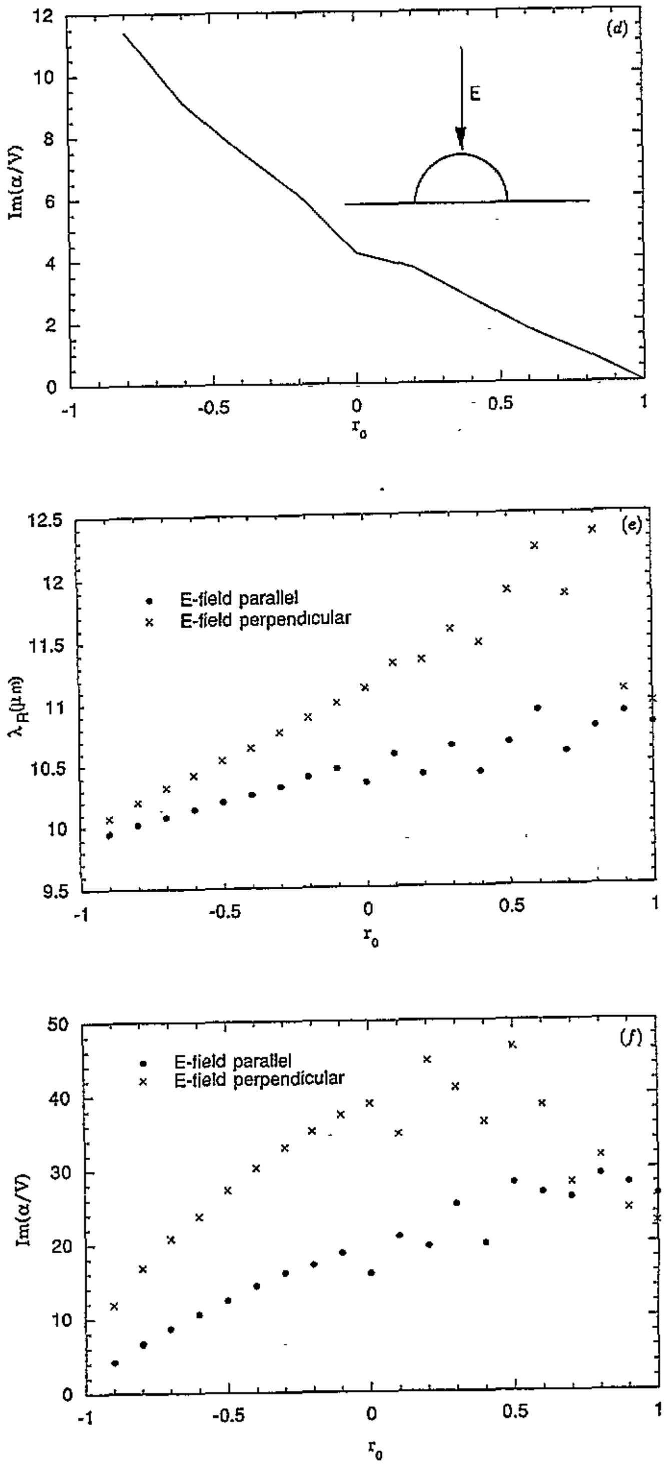

Figure 3. (Continued.) (d) The maximum imaginary polarizability per unit volume for the substrate-related resonance at ω_L in (c) versus r_0. (e) The resonance wavelength λ_R for the strongest Fröhlich-related resonances versus r_0. (f) The maximum imaginary polarizability per unit volume for the Fröhlich-related resonances in (e) versus r_0.

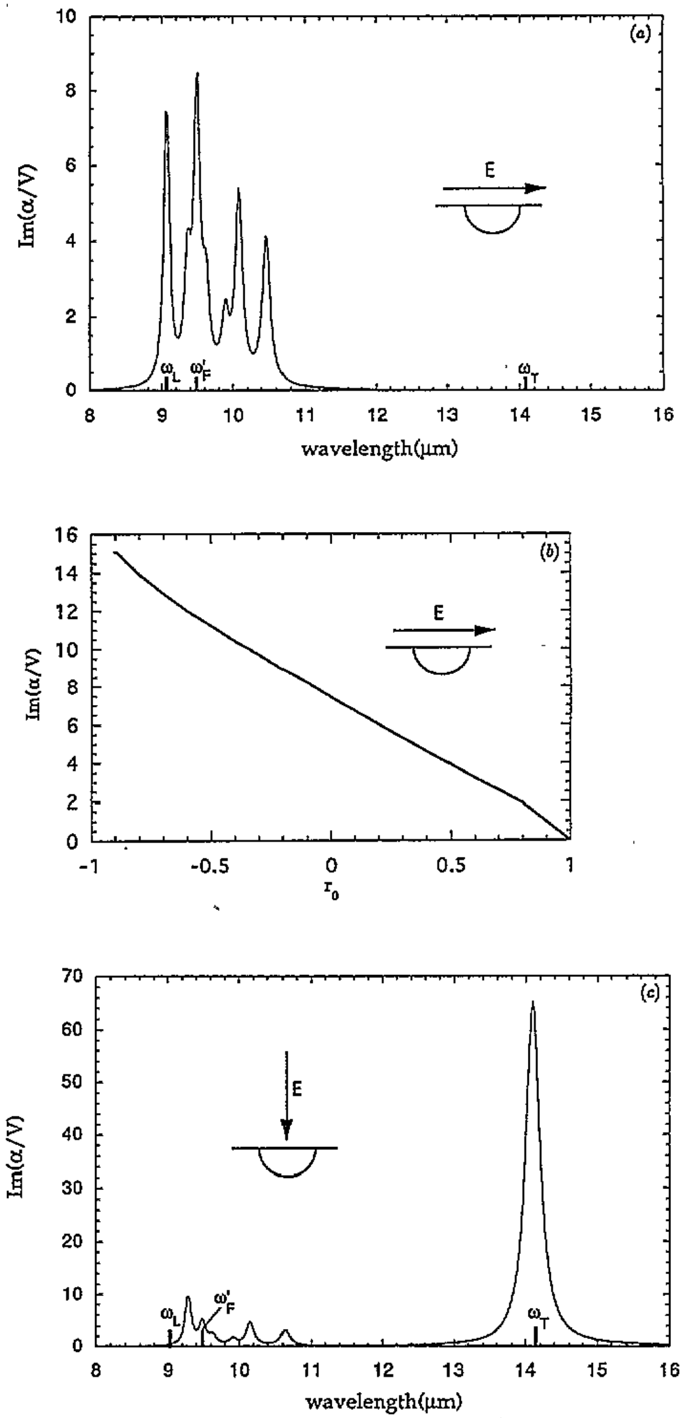

Figure 4. (a) The imaginary polarizability per unit volume versus wavelength (E parallel to the substrate) for a pit with $r_0 = 0$ at the surface of the substrate. (b) The maximum imaginary polarizability per unit volume for the substrate-related resonance at ω_L in (a) versus r_0. (c) The imaginary polarizability per unit volume versus wavelength (E perpendicular to the substrate) for a pit with $r_0 = 0$ at the surface of the substrate.

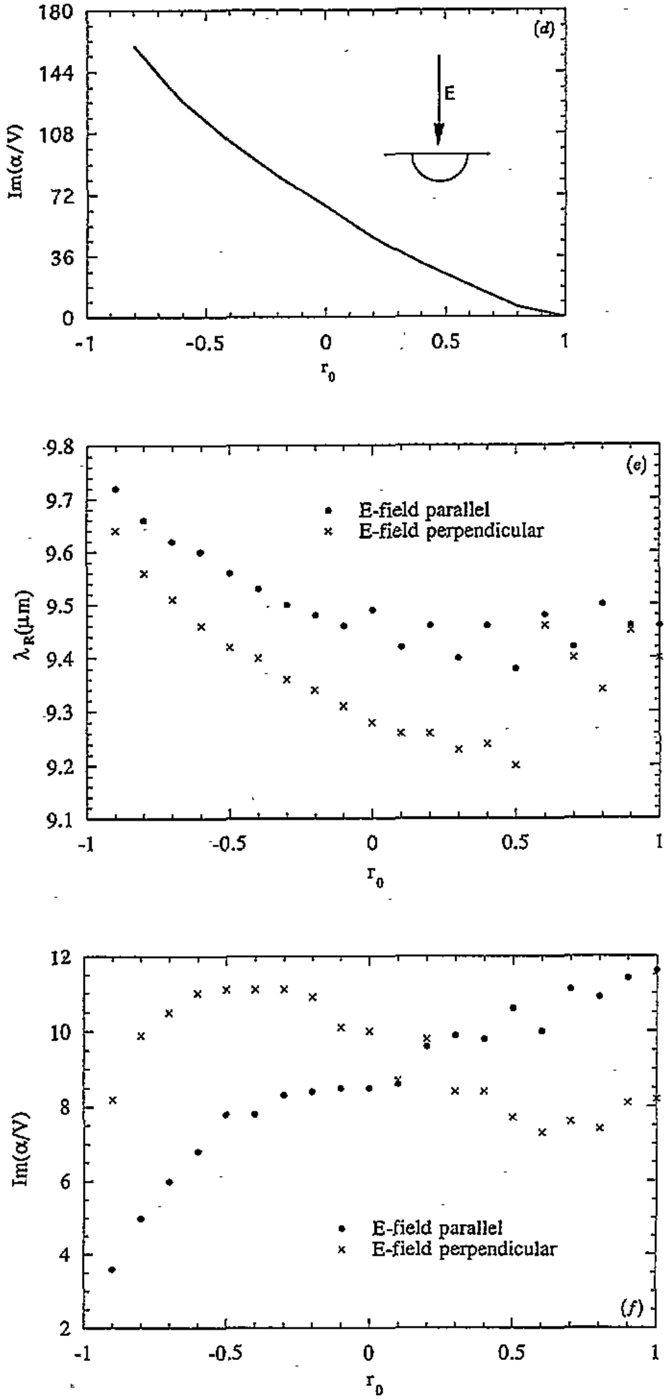

Figure 4. (Continued.) (d) The maximum imaginary polarizability per unit volume for the substrate-related resonance at ω_T in (c) versus r_0. (e) The resonance wavelength λ_R for the strongest Fröhlich-related resonances versus r_0. (f) The maximum imaginary polarizability per unit volume for the Fröhlich-related resonances in (e) versus r_0.

electric field, in sections 3.2–3.4. The imaginary part of the polarizability is proportional to the absorption. The wavelengths where $\mathrm{Im}(\alpha/V)$ has maxima can be understood as different resonance frequencies or phonon modes and the integrated area under each maximum gives the strength of the resonance.

3.2. Particle at the surface of the substrate

Consider a sphere at the surface of a substrate of the same material. We assume that the incoming light has normal incidence. A free sphere has a resonance mode at ω_F (see section 2.1) but, if the sphere is placed upon a substrate, several modes with different resonance frequencies can be excited. These resonances exist because of multipole interactions between the particle and the substrate.

Figure 2(a) shows that the imaginary polarizability per volume of a free beryllia sphere differs from that for a sphere in contact with the substrate. We observe three major resonance peaks if the beryllia sphere is in contact with the substrate. One of the peaks appears at the Fröhlich frequency of the free sphere at 10.4 μm, and the other two peaks appear because of interactions with the substrate. The strength of the resonances depends upon the damping in the material. However, the number of observable resonances may also depend on the damping factor. If the damping factor is high enough, the resonances overlap and cannot be distinguished from each other.

For oblate spheroids (see figure 2(b)) the peak at ω_F is smaller in magnitude and the peaks due to interactions with the substrate are stronger. The opposite is the case for a prolate spheroid (figure 2(c)). It is evident that the particle–substrate interaction becomes stronger when the particle centre is closer to the substrate surface.

In the following discussion we consider truncated spheres and holes in the surface of a substrate. They are used to model small bumps and pits.

3.3. Truncated spheres

Consider first a substrate with a smooth surface. The electric field E is parallel to the surface for normally incident light. E is the same in the substrate, at its surface, as in the ambient medium, because the tangential component of E is continuous. If the electric field is assumed to be constant, the displacement field D is very large for the resonance frequency ω_T.

It we now place a small sphere at the surface of the substrate the electric field distribution is much more complicated. Figure 2(c) shows that there exist three major resonance peaks for a beryllia sphere on a beryllia substrate, but there is no maximum of the imaginary polarizability at ω_T. However, if the sphere is truncated, there occurs a large resonance at the frequency ω_T of the transverse optical modem, as seen in figure 3(a). When the sphere is truncated, the large displacement field in the substrate 'leaks' into the particle and gives rise to a resonance in the particle–substrate system. In figure 3(b) we depict the value of $\mathrm{Im}(\alpha/V)$ at the resonance as a function of the truncation parameter. It is seen that the *resonance becomes stronger as the truncated sphere is flattened.*

Obliquely incident light has a component of the electric field that is perpendicular to the surface of the substrate. We now consider the case when E is perpendicular to the substrate. D is now the same in the substrate, at its surface, as in the surrounding medium, because the normal component of D is continuous. This means that the electric field just below the surface of the substrate is very large for the frequency ω_Lm, where the real part of the dielectric function is zero.

If a truncated sphere is present at the surface of the substrate, the electric field in the substrate 'leaks' into the particle. E inside the truncated sphere therefore becomes large at

ω_L and a resonance peak is observed, as seen in figure 3(c). This resonance occurs only because of the surface inhomogeneity. The effect is similar to the case when electromagnetic light at oblique incidence excites the longitudinal optical mode in a thin film [16]. The resonance becomes stronger as the truncated sphere is flattened (see figure 3(d)).

For both directions of the incident electric field, there occur several resonances between the TO and LO frequencies. One of them appears to be close to the Fröhlich frequency. We now study in particular the largest of the resonances between ω_T and ω_L. Figure 3(e) shows how its wavelength varies with the degree of truncation of the sphere. It is noted that the resonance wavelength decreases when the sphere is flattened. The convergence of the multipolar expansion is slow when the centre of the sphere lies above the surface of the substrate, as noted above. This is probably the reason for the scatter in the data for $r_0 > 0$. For $r_0 < 0$ the resonance wavelength is proportional to the truncation parameter, for E both parallel and perpendicular to the surface. When r_0 goes towards -1, the sphere is very flattened and the resonance wavelength goes towards 9.9 μm for the E both parallel and perpendicular to the surface.

The strength of the strongest 'Fröhlich-related' resonance varies with truncation parameter as shown in figure 3(f). The strength of the resonance decreases as the truncated sphere is flattened, for E both parallel and perpendicular to the surface.

3.4. Pits

Instead of a pit in the surface of the substrate, we consider a truncated sphere on a substrate with the dielectric constant $\epsilon' = \epsilon_m/\epsilon$ and surrounded by a medium with $\epsilon'_m = 1$.

We consider first the case of E parallel to the substrate. The imaginary part of the polarizability is depicted in figure 4(a). Because ϵ' has a maximum when $\epsilon = 0$, a strong resonance is seen at ω_L. The strength of the resonance increases as the truncation parameter r_0 decreases, as seen in figure 4(b).

The case when the electric field is perpendicular to the substrate is shown in figure 4(c). Here a resonance develops when $\epsilon' = 0$, i.e. at ω_T, when ϵ has a maximum. The value of $\mathrm{Im}(\alpha/V)$ at ω_T, as a function of the truncation parameter r_0, is shown in figure 4(d). It is notable that the strength of the substrate-related resonances depends upon the truncation parameter in a similar way for both bumps and pits. The strength of the resonances decreases continuously with r_0. The slope of the curve depends upon the damping of the TO absorption peak in the material. If the damping factor is increased, the slope of the curve decreases and vice versa. In addition, the substrate-related resonances are much stronger at ω_T than at ω_L, for both bumps and pits.

The Fröhlich frequency shifts to 9.4 μm for spherical holes. Figures 4(a) and 4(c) show that there exist a number of resonances in the vicinity of that frequency. The strongest Fröhlich-related resonance for pits is shifted as the truncation changes, as seen in figure 4(e). The shift is much smaller for pits than for bumps, and in the case of pits the resonance wavelength decreases as the truncation parameter r_0 increases.

The strength of the strongest 'Fröhlich-related' resonance is shown in figure 4(f). It is seen that the strength is quite low and decreases as the truncation parameter decreases, for both directions of E.

4. Summary

We have carried out a theoretical study of the effect of particles, bumps and pits at a surface on the infrared absorption in ionic materials. In this study we specifically consider BeO, but these absorption effects are general for all ionic or partly ionic materials.

We have shown that the multipolar interactions between the particle and the substrate give rise to several absorption peaks. We may distinguish two types of resonances. The first type occurs at ω_L or ω_T and is related to resonances in the substrate. Secondly, there exist resonances close to the Fröhlich frequency; these resonances are determined by the geometrical configuration of the particle–substrate system. The resonance frequencies are in general higher for pits in the surface than for bumps on the surface.

In experimental ceramic samples, the surface inhomogeneities are usually quite close packed. Hence realistic calculations should take into account multipolar interactions between the different particles and image multipoles. These interactions can be taken into account, for both lattices and random arrangements of particles [12], but a detailed study of these effects falls outside the scope of this paper. An interesting result of our calculations is that is should be possible to excite the longitudinal optical mode in surface inhomogeneities, using obliquely incident light.

Acknowledgments

We are grateful to Dr P Bobbert, University of Eindhoven, for providing us with a computer program for solving Laplace's equation and to Anders Larsson and Thomas Götschel who helped us with some finite-element method calculations. We appreciate illuminating discussions with Dr C G Ribbing. Economic support for this work was provided by The Swedish Natural Science Research Council and The National Defence Research Establishment.

References

[1] Ruppin R and Engelman R 1970 *Rep. Prog. Phys.* **33** 149–96
[2] Fröhlich H 1949 *Theory of Dielectrics* (London: Oxford University Press)
[3] Bohren C F and Huffman D R 1983 *Absorption and Scattering of Light by Small Particles* (New York: Wiley)
[4] Berreman D W 1967 *Phys. Rev.* **163** 855–64
[5] Ruppin R 1981 *Solid State Commun.* **39** 903–6
[6] Wind M M, Vlieger J and Bedeaux D 1987 *Physica* A **141** 33
[7] Wind M M, Bobbert P A, Vlieger J and Bedeaux D 1987 *Physica* A **143** 164
[8] Bobbert P A and Vlieger J 1987 *Physica* A **147** 115
[9] Andersson S K and Ribbing C G 1994 *Phys. Rev.* B **49** 11 336–43
[10] van de Hulst H C 1957 *Light Scattering by Small Particles* (New York: Dover)
[11] Magnus A P and Chauvaux R 1986 *Thin Solid Films* **142** 279–308
[12] Haarmans M T and Bedeaux D 1992 *Thin Solid Films* **224** 117–31
[13] Claro F 1984 *Solid State Commun.* **49** 229–32
[14] Smith G B, Vargas W E, Niklasson G A, Sotelo J A, Paley A V and Radchik A V 1995 *Opt. Commun.* **115** 8
[15] Palik E D 1991 *Handbook of Optical Constants of Solids II* (San Diego, CA: Academic)
[16] Berreman D W 1963 *Phys. Rev.* **130** 2193–8